



Laboratory Investigations into the Spectra and Origin of Propylene Oxide: A Chiral Interstellar Molecule

R. L. Hudson¹, M. J. Loeffler¹, and K. M. Yocum²

¹ Astrochemistry Laboratory (Code 691), NASA Goddard Space Flight Center, Greenbelt, MD 20771, USA; Reggie.Hudson@nasa.gov

² Department of Chemistry, Kutztown University, Kutztown, PA 19530, USA

Received 2016 September 12; revised 2016 December 13; accepted 2016 December 21; published 2017 January 31

Abstract

Propylene oxide was recently identified in the interstellar medium, but few laboratory results are available for this molecule to guide current and future investigations. To address this situation, here we report infrared spectra, absorption coefficients, and band strengths of solid propylene oxide along with the first measurement of its refractive index and a calculation of its density, all for the amorphous solid form of the compound. We present the first experimental results showing a low-temperature formation pathway for propylene oxide near 10 K in interstellar ice analogs. Connections are drawn between our new results and the interstellar molecules propanal and acetone, and predictions are made about several as yet unobserved vinyl alcohols and methylketene. Comparisons are given to earlier laboratory work and a few applications to interstellar and solar system astrochemistry are described.

Key words: astrobiology – astrochemistry – ISM: molecules – molecular data – molecular processes

1. Introduction

The recent discovery of propylene oxide in an interstellar cloud (McGuire et al. 2016) once more raises questions about the formation, evolution, and properties of such organic molecules in cold astronomical environments. However, studies of icy propylene oxide are severely hindered by the scarcity of relevant published information on this molecule. Therefore, we now report new laboratory investigations into propylene oxide's infrared (IR) spectra, low-temperature formation, reaction products, and selected physical properties. These new results will be useful in guiding future work and in understanding the conditions under which propylene oxide can form and evolve.

Propylene oxide (PrO, C₃H₆O), also known as epoxy propane and methyloxirane, is a cyclic ether of special significance because it is the first chiral interstellar organic molecule identified, chiral referring to the fact that the molecule cannot be superimposed on its mirror image. See the mirror-image structures in Figure 1. Chirality is of particular interest since terrestrial biochemistry often favors only one member of a mirror-image pair for biological activity, such as with amino acids and sugars. In most cases, the two members of a mirror-image pair have identical chemical and physical properties, with the direction of rotation of plane-polarized light being the most famous exception for chiral molecules.

In recent years we have studied many small organic molecules in our laboratory, characterizing amorphous and crystalline forms of molecular ices and measuring IR band strengths at 10–150 K. We have published results on five nitriles for the study of Titan's atmosphere, new spectra of CO₂ and CH₄ for interstellar studies, and new results on C₂H₂, C₂H₄, and C₂H₆ for application to trans-Neptunian objects (Moore et al. 2010; Hudson et al. 2014a, 2014b; Gerakines & Hudson 2015a, 2015b). We have generated new, and in some cases the first, IR spectra of the amorphous phases of these compounds, and corrected problems and contradictions in the literature that have persisted for several decades and influenced both interstellar and planetary investigations. Here we extend

our efforts to propylene oxide, with two tasks in mind. First, we present new IR spectra, the first IR band strengths, and selected physical properties for solid PrO to guide this and future work. Second, we describe a low-temperature reaction path to make PrO, supported by new laboratory experiments and having potential applications to the study of interstellar ices, trans-Neptunian objects, and other solar system objects, including the Moon, comets, icy satellites, and possibly meteorites.

2. Experimental Methods

Most of the methods and equipment employed were as described in our recent papers. The main exception was that IR spectra for measuring band strengths were recorded with a new Thermo iS50 spectrometer over 6000–500 cm⁻¹ (1.67 to 20.0 μm) with 2 cm⁻¹ resolution and 100 accumulations per spectrum. Equipment for measuring refractive indices at 670 nm and for recording spectra before and after ion irradiations was the same as before (e.g., Moore et al. 2010; Hudson et al. 2014a; Loeffler et al. 2016a).

Ice samples were prepared by deposition of a vapor (or gas) onto a pre-cooled substrate (area ≈ 5 cm²) at a rate that gave an increase in the ice's thickness of a few micrometers per hour, as determined by recording interference fringes (Groner et al. 1973), and a final thickness of 0.3–3 μm. For radiation experiments, the substrate was polished aluminum, and the IR spectra were recorded in a transmission–reflection–transmission mode with the IR beam a few degrees from a perpendicular to the substrate and sample. In all other cases the substrate was KBr with spectra recorded in a standard transmission configuration. Repeated tests with several resolutions and ices of different thicknesses ensured that propylene oxide's spectral features were neither saturated nor resolution limited. Also, appropriate blank (control) experiments were carried out to check that the spectral changes we observed in irradiated ices did not appear in unirradiated samples on warming. Mixtures of PrO and CO₂ were studied with the CO₂: PrO ratio varying from about 1:1 to 20:1, but without significant differences in the products observed.

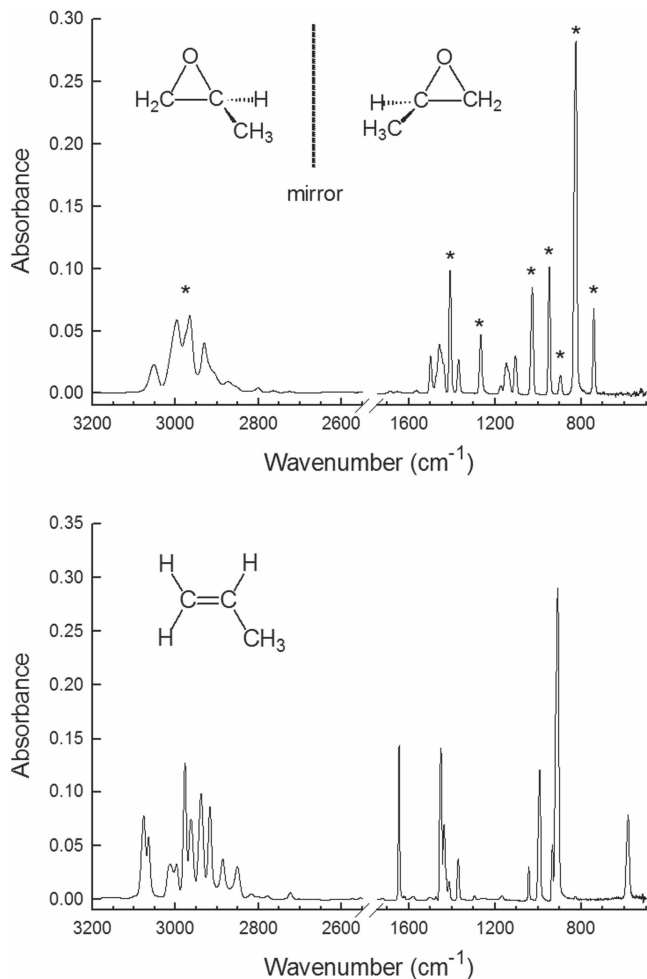


Figure 1. Infrared survey spectra of amorphous solids at 10 K. Top: a propylene oxide sample with a thickness of about $1.3 \mu\text{m}$. Asterisks indicate the features listed in Table 1. In the two mirror-image structures, the C–H bond drawn with dashes is pointing behind the plane of the OCC triangle while the darker C–CH₃ bond is pointing in front of the same plane. Bottom: a propylene sample with a thickness of about $1.3 \mu\text{m}$.

The ice samples we studied were prepared by either a background deposition or deposition from a capillary-array type doser to ensure a uniform coating of the substrate, but no evidence was found that the deposition method influenced our results. Other ice formation techniques, such as ballistic deposition from a single tube, could give slightly different values for certain physical properties of the ices (Loeffler et al. 2016b), but the radiation chemistry should remain the same, specifically propylene oxide formation as we describe.

Our radiation source was a beam of protons ($p+$) from a Van de Graaff accelerator at a current of about 1×10^{-7} A and an energy of 0.924 MeV (Loeffler et al. 2016a). Since the calculated (Ziegler 2013) ranges of 0.924 MeV protons were 20–30 μm , depending on the sample’s initial composition, and since our ices were only a few micrometers in thickness, the incident protons passed through our ices and came to a stop in the underlying aluminum substrate. The resulting current there was detected and integrated with an electrometer to give the incident radiation fluence F (in $p+ \text{cm}^{-2}$). Stopping powers (S) of 0.924 MeV protons in our samples were computed with Ziegler’s SRIM program (Ziegler 2013). We calculated $S = 279 \text{ MeV cm}^2 \text{ g}^{-1} p+^{-1}$ for propylene oxide, using a

density (ρ) of 0.754 g cm^{-3} (see below). For CO₂-rich ice mixtures containing propylene, meaning all for which we show spectra here, we used the calculated stopping power, and measured density and refractive index, for pure CO₂: $S = 224 \text{ MeV cm}^2 \text{ g}^{-1} p+^{-1}$, $\rho = 1.15 \text{ g cm}^{-3}$, $n = 1.26$ (Loeffler et al. 2016b).

Absorbed radiation doses in SI units of gray (Gy) were found from $SF \times (1.60 \times 10^{-10} \text{ Gy g MeV}^{-1})$, from which doses in the older units of megarads (Mrad) were obtained from $1 \text{ MGy} = 100 \text{ Mrad}$. Absorbed doses in the non-standard, but convenient, “eV molecule⁻¹” unit are sometimes encountered in the astrochemical literature, and are simply $m_{\text{avg}} SF$, where m_{avg} (in grams) is the average mass of a molecule in the ice sample. This means that for propylene oxide an incident proton fluence of $F = 1 \times 10^{14} p+ \text{cm}^{-2}$ delivered an absorbed dose of $4.46 \text{ MGy} = 446 \text{ Mrad} = 2.69 \text{ eV molecule}^{-1}$. Similarly, for CO₂-rich ices an incident fluence of $F = 1 \times 10^{14} p+ \text{cm}^{-2}$ corresponds to $3.58 \text{ MGy} = 358 \text{ Mrad} = 1.64 \text{ eV molecule}^{-1}$, using the stopping power of pure CO₂. These conversions will be used for all experiments in this paper. See Gerakines & Hudson (2013) for further discussion of radiation units.

In a few cases we computed infrared ¹⁸O isotopic shifts to confirm spectral assignments. These calculations were done with the Spartan (Wavefunction) program using density functional theory (DFT) at the B3LYP/6–311+G** level. No scaling factors were applied to the results.

All reagents were obtained from Sigma Aldrich, with purities of 99% or higher, and were used as received except for the degassing of propylene oxide by several liquid nitrogen freeze-pump-thaw cycles.

3. Results

3.1. Refractive Indices and Density

Values of the refractive index and density of solid propylene oxide were needed to determine ice thicknesses and IR band strengths, but were not found in the literature. Therefore, we used two-laser interferometry (Tempelmeier & Mills 1968) to measure the refractive index at 670 nm of PrO ices made by vapor-phase deposition. The average of three measurements at 17 K was $n = 1.329 \pm 0.004$, where the uncertainty is the standard error determined from the standard deviation. For PrO’s density, the Lorentz–Lorenz equation was used in the form

$$\rho = \left(\frac{1}{r}\right) \left(\frac{n^2 - 1}{n^2 + 2}\right) \quad (1)$$

where r is the specific refraction of propylene oxide. With $\rho = 0.829 \text{ g cm}^{-3}$ and $n = 1.366$ for PrO at 20 °C (Holden 1952), we calculated $r = 0.270 \text{ cm}^3 \text{ g}^{-1}$, and then reversed the process to use Equation (1) to calculate $\rho(10 \text{ K}) = 0.754 \text{ g cm}^{-3}$ from our measured n value. Since little information is available on either n or ρ at these temperatures, we also measured n for ethylene oxide (EtO), obtaining $n(17 \text{ K}) = 1.324 \pm 0.006$, again for three determinations. Near room temperature $n(\text{EtO}) \approx n(\text{PrO})$, and our measurements showed that they are indeed nearly the same also at 17 K.

Table 1
Infrared Absorptions of Amorphous Propylene Oxide at 10 K

Peak Position (cm ⁻¹)	α' (cm ⁻¹) ^a	Integration Range (cm ⁻¹)	A' (10 ⁻¹⁸ cm molec ⁻¹) ^b	Approximate Description ^c
2965.8	1096	3100.0–2830.0	11.53	CH, CH ₂ , CH ₃ stretches
1408.2	1651	1424.0–1386.6	2.57	CH ₃ deformation
1266.0	808	1290.0–1235.0	1.47	ring deformation
1027.3	1430	1050.0–1015.0	2.46	CH ₃ wagging
948.3	1727	970.0–925.0	2.35	CH ₃ rocking
896.7	257	920.0–875.0	0.48	ring deformation or CH ₂ rocking
825.9	4864	860.0–789.6	9.53	ring deformation
742.0	1093	770.8–714.4	1.43	ring deformation or CH ₂ rocking

Notes.

^a From the slopes of Beer's Law graphs of $2.303 \times$ (peak height) against ice thickness. In each case, the slope is the apparent absorption coefficient, α' .

^b From the slopes of Beer's Law graphs of $2.303 \times$ (band area) against ice thickness. In each case, the slope divided by $(\rho N_A / MW)$ gives A' , where MW = molecular weight = 58.08 g mol⁻¹, $N_A = 6.022 \times 10^{23}$ molecules mol⁻¹, and density = 0.754 g cm⁻³. For recent examples see Gerakines & Hudson (2015a).

^c From Tobin (1960). Gontrani et al. (2014) have more accurate, more complex descriptions.

3.2. Infrared Spectra of Propylene Oxide

To our knowledge, the IR spectrum of solid propylene oxide has not been published. The upper panel of Figure 1 shows the transmission spectrum of PrO (ice thickness $\approx 1.3 \mu\text{m}$) deposited at ~ 10 K onto a KBr substrate. Of the many features shown, the eight regions marked by asterisks, and listed in Table 1, were selected for study. Beer's law plots were constructed for these features by measuring peak heights and band areas as a function of ice thickness. The slopes of the resulting graphs, combined with our n and ρ values, gave apparent absorption coefficients (α') and band strengths (A'), and these also are included in Table 1. Note that all such tabulated values were multiplied by 2.303 to convert from the base-10 to the base-e scale needed for optical depth. See Hollenberg & Dows (1961) or our recent papers for additional details (e.g., Gerakines & Hudson 2015b). Table 1's comments on the motions associated with each vibration are from Tobin (1960), but see Gontrani et al. (2014) for more-accurate descriptions.

Slowly warming the sample, which is represented in the upper panel of Figure 1, from 10 to 90 K scarcely changed its spectrum, but at 90–95 K the initially rounded and relatively featureless peaks sharpened and were accompanied by splittings and slight shifts in position. These observations indicated that the ice initially was an amorphous solid, the spectral changes seen by 95 K being due to its crystallization. Continued warming gave subtle additional changes at 110–115 K, suggesting that a second phase change occurred, this time a crystalline–crystalline transition. Neither crystalline form was obtained to the exclusion of the other by warming an amorphous sample, but the individual low- and high-temperature crystalline phases could be prepared directly by depositing at 100 and 120 K, respectively. Spectra of the two crystalline phases were distinct, but not dramatically different, suggesting a similarity reminiscent of that between metastable and crystalline forms of ethylene previously observed (Hudson et al. 2014b). Although the crystalline phases of propylene oxide are inherently interesting, our goal was to characterize and recognize them so as to avoid them and instead to focus on the more astrochemically relevant amorphous form of the compound. All changes on warming PrO were irreversible, and all samples sublimed in our vacuum system in a few minutes at 135 K.

The lower panel of Figure 1 shows the infrared spectrum of amorphous propylene (C_3H_6 , $\text{H}_2\text{C}=\text{CH}-\text{CH}_3$) near 10 K, to which we return in the next section.

3.3. Low-temperature Syntheses—Radiation Chemistry

Molecules with three-membered OCC rings, such as PrO (Figure 1), are termed epoxides and the reactions that form them are called epoxidations. The standard laboratory method for making epoxides involves organic peracids (Prileschajew 1909), although newer and more elegant epoxidation procedures exist (e.g., Katsuki & Sharpless 1980). However, such laboratory syntheses are unlikely sources of epoxides in cold interstellar or planetary environments. Since ices in many such astronomical environments are exposed to ionizing radiation, such as cosmic rays, magnetospheric electrons, and vacuum-UV photons, we focused our attention on the possible radiation–chemical synthesis of propylene oxide.

We began with a baseline experiment that helped with later work, a $p+$ irradiation of amorphous propylene oxide at 20 K. Irradiation to a fluence of $2 \times 10^{15} p+ \text{cm}^{-2}$ gave an IR spectrum displaying substantial increases in absorbance at 3600–3100 cm⁻¹ and near 1720 cm⁻¹ due to the formation of compounds with hydroxyl (O–H) and carbonyl (C=O) functional groups, respectively. Sharp peaks appearing near 2338, 2136, and 1302 cm⁻¹ were from CO₂, CO, and CH₄, respectively. More significantly, small but distinct peaks of propylene (lower panel, Figure 1) grew in at 1644 and 917 cm⁻¹ during the irradiation. Warming the irradiated ice removed the CO₂, CO, and CH₄ features, but did little else except for one interesting exception. Warming to ~ 150 K removed CO and revealed a well-resolved, symmetrical peak nearby at 2113 cm⁻¹, which we assigned to methylketene for reasons described below. Firm identifications for other reaction products, such as hydrocarbons, ethers, and alcohols, were not pursued for this initially one-component ice.

The work just described was a degradation experiment showing that ionizing radiation reduces propylene oxide ($\text{C}_3\text{H}_6\text{O}$) to propylene (C_3H_6). This suggested that solid PrO might form in a cold interstellar cloud, and in laboratory ices, through the reverse process, $\text{O} + \text{C}_3\text{H}_6 \rightarrow \text{C}_3\text{H}_6\text{O}$. The requirements are a source of O atoms to combine with propylene to open the hydrocarbon's double bond and give the three-membered ring of PrO. Many O-atom sources can be envisioned (e.g., N₂O, NO₂, H₂O₂, O₃), but from an

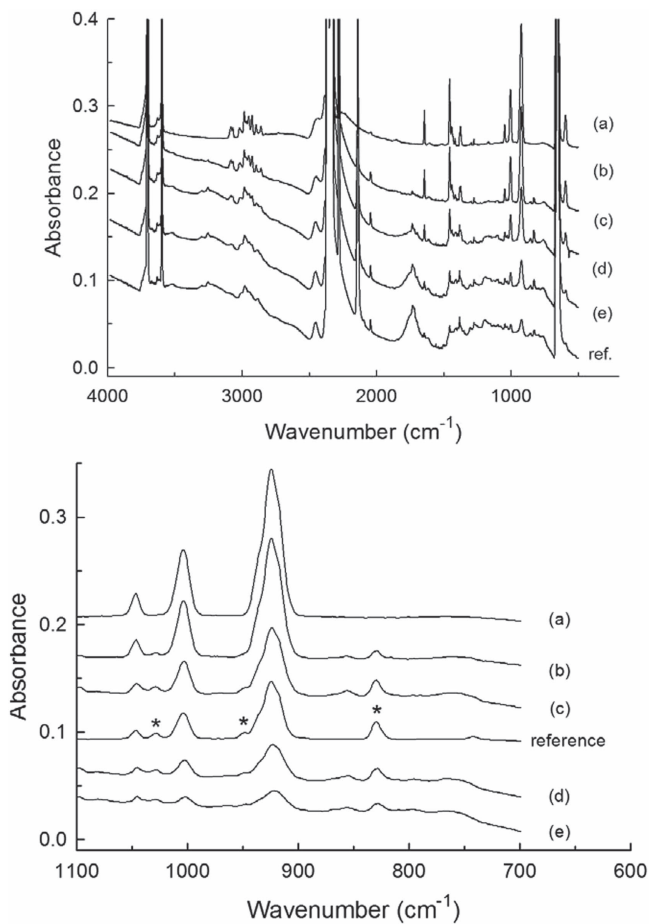


Figure 2. Infrared spectra of $\text{CO}_2 + \text{propylene}$ (13:1) at 10 K before and after irradiation. The radiation fluencies were (a) 0, (b) $1.2 \times 10^{13} p+ \text{cm}^{-2}$, (c) $4.6 \times 10^{13} p+ \text{cm}^{-2}$, (d) $9.3 \times 10^{13} p+ \text{cm}^{-2}$, and (e) $14 \times 10^{13} p+ \text{cm}^{-2}$. The conversion to absorbed dose is $4.6 \times 10^{13} p+ \text{cm}^{-2} \approx 1 \text{ eV molecule}^{-1}$. The reference spectrum is from an unirradiated ice with composition $\text{CO}_2 + \text{C}_3\text{H}_6 + \text{C}_3\text{H}_6\text{O}$ ($\sim 10:1:0.1$), scaled to roughly match the PrO peaks in (c).

astrochemical vantage point solid CO_2 is a particularly attractive choice as it is found in both planetary and interstellar environments. Both ionizing radiation and far-UV photons can break a $\text{C}=\text{O}$ bond in a CO_2 molecule to give $\text{CO}_2 \rightarrow \text{CO} + \text{O}$ with the O atom being available for subsequent reaction.

Figure 2's upper panel shows IR spectra of a $\text{CO}_2 + \text{C}_3\text{H}_6$ ice mixture (13:1) at 10 K before and after irradiation with $\sim 0.9 \text{ MeV } p+$. An absorbance increase in the 1700 cm^{-1} region on proton irradiation can again be attributed to the formation of carbonyl-possessing molecules. Absorbance changes at $3600\text{--}3100 \text{ cm}^{-1}$ again suggested the synthesis of molecules with OH groups. Unfortunately, in all cases the complexity of the IR spectra was such that little further information was gleaned from warming any of these irradiated ices. Aside from the loss of CO_2 , CO , and CH_4 , nearly all IR features persisted until at least 150 K, and no distinct new ones appeared. As with neat propylene oxide, warming the irradiated $\text{CO}_2 + \text{C}_3\text{H}_6$ ice removed the CO fundamental at 2136 cm^{-1} , revealing a small symmetrical peak near 2113 cm^{-1} .

The PrO positions in Table 1 and Figure 1 can be compared to the spectrum of either unirradiated C_3H_6 (Figure 1, lower panel) or $\text{CO}_2 + \text{C}_3\text{H}_6$ (Figure 2, upper panel, trace a) to determine the IR regions in which radiation-synthesized PrO might be identified. Absorbances of PrO near 2950 and 1400

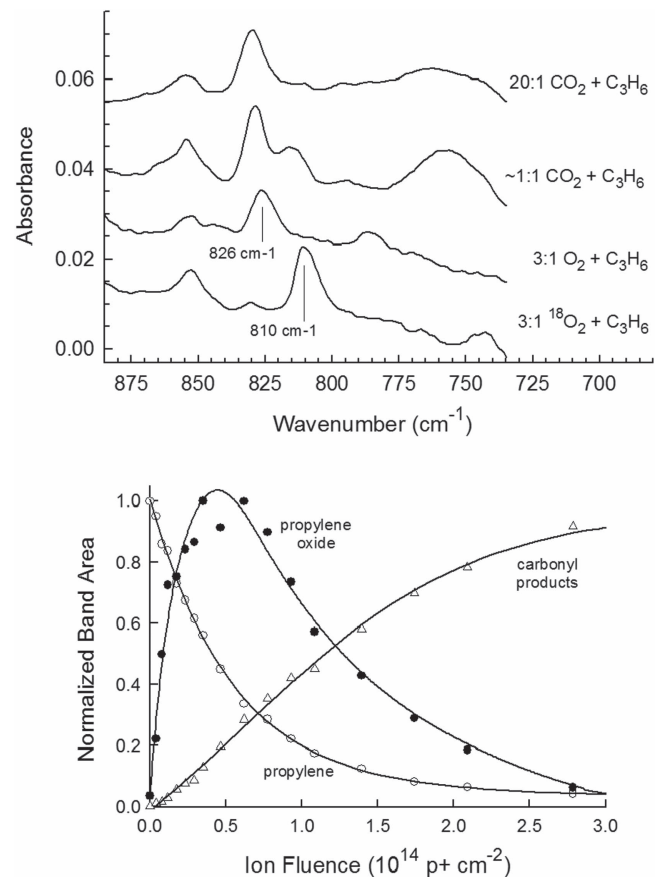


Figure 3. Upper: propylene oxide feature near 826 cm^{-1} in four different irradiated ices, the radiation fluence being about $5 \times 10^{13} p+ \text{cm}^{-2}$ in each case. Lower: relative changes in propylene oxide's abundance (826 cm^{-1} band) during proton irradiation of $\text{CO}_2 + \text{propylene}$ ($\sim 20:1$) at 10 K, also showing the decrease in abundance of the reactant propylene (923 cm^{-1} band) and the rise in abundance of carbonyl products (1730 cm^{-1} band).

cm^{-1} will be obscured by C_3H_6 , leaving the intense PrO feature near 826 cm^{-1} as the best candidate. The lower panel of Figure 2 shows an expansion of this region, and indeed an IR feature near 826 cm^{-1} is seen to rise and then fall with increasing radiation dose. This peak is assigned to PrO as are two others, marked with asterisks, near 1027 and 948 cm^{-1} . A reference spectrum of unirradiated $\text{CO}_2 + \text{C}_3\text{H}_6 + \text{PrO}$ is shown for comparison.

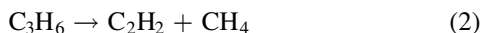
Figure 3's upper panel shows the result of changing several variables in our radiation experiments, but with each ice receiving the same incident fluence ($F = 5 \times 10^{13} p+ \text{cm}^{-2}$). Going from top to bottom, the uppermost trace shows the strongest PrO peak is present after irradiation of a $\text{CO}_2 + \text{C}_3\text{H}_6$ ($\sim 20:1$) sample, while the second spectrum shows that it remains prominent in an irradiated ice with a much larger initial abundance of C_3H_6 ($\sim 1:1$). The third and fourth spectra in this panel show that the same PrO feature was present when the oxygen source was changed from CO_2 to O_2 , and that a shift of $826\text{--}810 = 16 \text{ cm}^{-1}$ resulted when $^{18}\text{O}_2$ was used in the experiment, close to the 15 cm^{-1} predicted by a density functional calculation for propylene oxide.

In related experiments, an ice sample made of $^{16}\text{O}_2 + ^{18}\text{O}_2 + \text{C}_3\text{H}_6$ ($\sim 1.5:1.5:1$) was irradiated and its spectrum showed the 826 and 810 cm^{-1} peaks that we assigned to Pr^{16}O and Pr^{18}O , respectively, and with no other IR peak between them. The same $\sim 15 \text{ cm}^{-1}$ isotopic shift was

seen in irradiated $\text{C}^{18}\text{O}_2 + \text{C}_3\text{H}_6$ ($\sim 20:1$) ices, and when a sample consisting of $\text{C}^{16}\text{O}_2 + \text{C}^{16}\text{O}^{18}\text{O} + \text{C}^{18}\text{O}_2 + \text{C}_3\text{H}_6$ ($\sim 5:10:5:1$) was irradiated, the only IR peaks observed were the two just mentioned. These ^{18}O experiments supported our assignment of the band near 826 cm^{-1} to propylene oxide, a molecule with a single oxygen atom. Other PrO absorbances were either too weak or too obscured by other bands to determine reliable isotopic shifts.

The lower panel of Figure 3, again from irradiated $\text{CO}_2 + \text{C}_3\text{H}_6$, shows that during a radiation experiment the abundance of the propylene reactant decreased exponentially, PrO's abundance rose and then fell, and that there was a monotonic increase in carbonyl ($\text{C}=\text{O}$) absorbance. The maximum abundance of PrO made was estimated by preparing $\text{CO}_2 + \text{C}_3\text{H}_6 + \text{PrO}$ ices and comparing the intensities of their IR bands to those from irradiated $\text{CO}_2 + \text{C}_3\text{H}_6$ samples having the same thickness. From such comparison spectra, and the reduction in the initial propylene abundance on irradiation, the propylene oxide yield for the experiment in Figure 2 was estimated to be about 10%.

As already stated, our interest was much more focused on the formation of PrO than on its destruction and its reaction products. Nevertheless, several product identifications were made. Perhaps of most interest, IR spectra of our irradiated $\text{CO}_2 + \text{C}_3\text{H}_6$ ices gave peaks at 1736 , 1699 , and 853 cm^{-1} that were matched by propanal (propionaldehyde), $\text{HC}(\text{O})\text{CH}_2\text{CH}_3$, trapped in solid CO_2 . A small absorbance between the 1736 and 1699 cm^{-1} peaks was close to acetone's carbonyl feature near 1718 cm^{-1} , but was too weak for a firm assignment. Three peaks for propyne (C_3H_4 , methyl acetylene) were found in these irradiated samples (2133 , 853 , and 764 cm^{-1}) as were two from its allene isomer (1948 , 850 cm^{-1}), all verified by comparison to reference spectra of each compound in a CO_2 -rich ice mixture. The radiolytic decomposition of propylene (C_3H_6) as



might be expected to make both acetylene (C_2H_2 , $\sim 758\text{ cm}^{-1}$) and methane (CH_4 , $\sim 1300\text{ cm}^{-1}$; Hudson et al. 2015), but IR peaks at these positions were broad and weak, again leading to only tentative assignments and the conclusion that reaction (2) was of little importance in these experiments. With appropriate reference spectra of unirradiated ices rich in CO_2 it should be possible to continue this approach and make reasonably firm assignments to other IR features, a task we leave to the future.

A final radiation experiment was with solid propylene. Expected reaction products, such as propyne, acetylene, and methane, were observed. Again, although this experiment has some inherently interesting features, we treated it as a control (blank) to see if any of the IR peaks we attribute to propylene oxide were observed in this oxygen-free sample. They were not.

4. Discussion

4.1. Spectra, Properties, and Reactions

Our IR spectra of amorphous propylene oxide agree with expectations from the spectra of liquid, gaseous, and matrix-isolated PrO published by, among others, Tobin (1960) and Gontrani et al. (2014). The sharpening, new splittings, and spectral shifts seen on crystallization are from the adherence of

the amorphous and crystalline ices to different sets of selection rules. The existence of two crystalline phases for propylene oxide is consistent with the report of two phases for ethylene oxide (Schriver et al. 2004). No publications seem to be available to compare with our measurements of α' and A' . These quantities can be useful in quantifying photochemical studies of the formation or destruction of PrO in icy solids and, in the absence of a full set of optical constants (n and k), can be used to approximate near- and far-IR band strengths for PrO by comparing band intensities in those regions with our mid-IR results in Table 1.

Multiple lines of evidence support epoxidation in $\text{CO}_2 + \text{C}_3\text{H}_6$ ices as the correct interpretation of our radiation-chemical work. First, the features assigned to PrO in our IR spectra of irradiated samples agree with reference CO_2 -rich ice mixtures containing that compound. Second, the observed ^{18}O isotopic shift matches the DFT-calculated shift for PrO's band near 826 cm^{-1} . Third, an independent synthesis in which O_2 was substituted for CO_2 gave the same PrO IR features. Fourth, our results fully agree with chemical expectations for the scavenging of O atoms by an unsaturated hydrocarbon, propylene in this case.

Our radiation results can be explained through the work of Cvetanović (1958) on alkenes, hydrocarbons with a $\text{C}=\text{C}$ double bond. For the simpler case of ethylene oxide, Figure 4 shows the key steps for making $\text{C}_2\text{H}_4\text{O}$ isomers, starting with O-atom addition to ethylene ($\text{H}_2\text{C}=\text{CH}_2$) to form a diradical (two unpaired electrons), which in turn can undergo ring closure to make product (a), ethylene oxide. Alternatively, two possible paths of H-atom transfer within the diradical, followed by bond formation, lead to (b) acetaldehyde and (c) vinyl alcohol. All three of these product molecules are reported to be interstellar (Gilmore et al. 1976; Dickens et al. 1997; Turner & Apponi 2001).

Figure 5 shows that a similar scheme for our experiments involving the addition of oxygen to propylene is considerably more complex. The non-equivalence of the two numbered carbon atoms leads to the products shown in Scheme 1 and Scheme 2. Both yield PrO, but one scheme also leads to (b) propanal whereas the other leads to (e) acetone, again both being known interstellar molecules. The remaining products expected, (c) and (f), are methyl-substituted vinyl alcohols for which little data are available. Products (b) and (e) have carbonyl groups ($\text{C}=\text{O}$) and explain the increase in absorbance seen near 1720 cm^{-1} in our ices on irradiation, while alcohol products (c) and (f), with OH groups, probably contribute to the absorbance increase observed at $3600\text{--}3100\text{ cm}^{-1}$ in Figure 2. Similar comments apply to our irradiation of neat PrO. Propylene oxide suffers from substantial strain energy, and so electronic excitation can readily break a $\text{C}-\text{O}$ bond of (a) in Scheme 1, or (d) in Scheme 2, returning one to the diradical from which the other products can form. In fact, this is the likely explanation for the initial rise in PrO's abundance and its subsequent fall on further irradiation (Figure 3, bottom), the reaction sequence from propylene to propanal being as follows:



Other PrO isomers could be involved in these reactions, but no firm evidence for them was found in our work; their formation would be more complicated than what we consider in Figure 5, and activation energies to reach them are likely to be larger

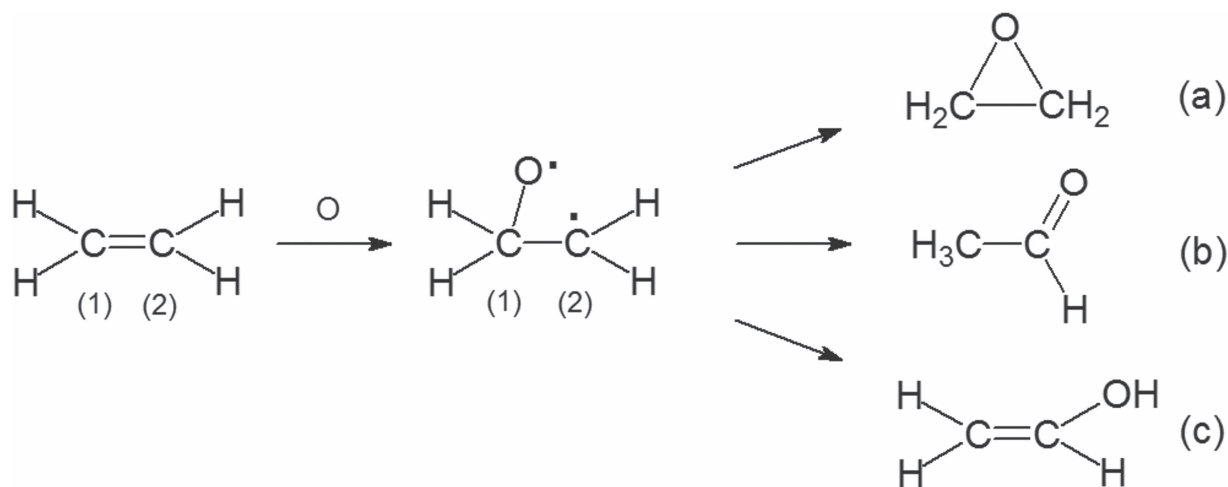
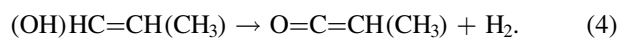


Figure 4. Oxygen-atom addition to ethylene leads to a diradical and from it to three product molecules, (a) ethylene oxide, (b) acetaldehyde, and (c) vinyl alcohol. Modified from Cvetanović (1958).

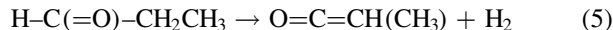
than for the products we considered (e.g., calculations of Dubnikova & Lifshitz 2000). As a small point, our difficulty in detecting acetone, Figure 5’s product (e), compared to the ease of detecting propanal, Figure 5’s product (b), may reflect a lower acetone yield due to partial blocking of an approaching O atom from the reaction site by the methyl ($-\text{CH}_3$) group at carbon (2). Additional work is needed to explore this possibility.

The reaction sequences in Figures 4 and 5 are reasonable, but they should not be interpreted as complete reaction mechanisms. Many details remain unknown, such as whether or not the changes shown occur in a concerted or a step-wise manner, or even whether PrO isomerization might not proceed by electronic excitation without the need for a biradical intermediate. In general, it is unusual to be able to determine such mechanistic details in irradiated-ice experiments as there are few in situ methods to examine reactive intermediates and reaction products. Irradiated samples can be warmed and mass spectrometric techniques used to detect gas-phase species released, and various chromatographic methods can be used to analyze melted ices at room temperature, but the resulting phase and energy changes can alter composition. These difficulties are significant when trying to understand reaction chemistry in interstellar ice analogs (e.g., 10–50 K), but perhaps less so in other cases, such as in experiments to determine reaction products released when ices are warmed in interstellar clouds.

A final point concerns the weak IR feature near 2113 cm^{-1} seen after irradiating and warming both PrO and $\text{CO}_2 + \text{C}_3\text{H}_6$ ices. This peak was assigned to methylketene, $(\text{CH}_3)\text{HC}=\text{C}=\text{O}$, based on our starting materials, the band’s position, its tendency to remain in the spectrum on warming to about 150 K, and our experience with ketene (Hudson & Loeffler 2013). Also, the 16 cm^{-1} difference we found between ketene (Hudson & Loeffler 2013) and methylketene in the solid state matches that between these same two molecules in the gas phase (Kwiatkowski & Leszczyński 1995; Winther et al. 2002). The work of Hawkins & Andrews (1983) suggests that methylketene was made by H_2 elimination from a precursor vinyl alcohol with a $(\text{OH})\text{HC}=\text{C}$ grouping, such as (c) from Figure 5 and the following reaction:



Alternatively, or in addition to reaction (4), the solid-phase elimination of H_2 from propanal as



will give methylketene. In no case was evidence for the parent ketene ($\text{H}_2\text{C}=\text{C}=\text{O}$) found in our experiments, although ketene has been known to be a decomposition product of many simple organic molecules for over a century (Wilsmore & Stewart 1907).

4.2. Relationship to Previous Work

For the most part, our propylene oxide results mirror those obtained from EtO and its isomers. Schriver et al. (2004) showed that low-temperature UV photolysis of EtO produces acetaldehyde and ketene, which agrees with our observation of the formation of carbonyl-possessing molecules and methylketene from propylene oxide. Bennett et al. (2005) studied the electron irradiation of $\text{CO}_2 + \text{C}_2\text{H}_4$ ices near 10 K, showing that acetaldehyde and ethylene oxide were produced, again in agreement with the experiments reported here. Somewhat earlier, our own work linked these same molecules with vinyl alcohol (Hudson & Moore 2003). These three studies of $\text{C}_2\text{H}_4\text{O}$ molecules assisted the present investigation of $\text{C}_3\text{H}_6\text{O}$ isomers, but an extension along this homologous series to the $\text{C}_4\text{H}_8\text{O}$ family is likely to be challenging due to the larger number of isomers possible.

Beyond these papers from the astrochemical literature are several older matrix-isolation studies, such as the UV photolyses of propylene isolated in argon (Guillory & Thomas 1975) and of $\text{O}_3 + \text{propylene}$ trapped in argon (Coleman & Ault 2010), and also the thermal chemistry of $\text{O}_3 + \text{propylene}$ mixtures trapped in xenon (Andrews & Kohlmeier 1982). To the extent that comparisons are possible, our work is consistent with all of these studies, but differs in not using rare-gas matrices. The latter can be invaluable for elucidating reaction pathways, but are not meant to be representative of either interstellar or planetary ices.

More recent than the work just described is that of Ward, Price, and colleagues who investigated the formation of both ethylene oxide and propylene oxide on unirradiated graphite, which served as an interstellar dust analog (Ward & Price 2011;

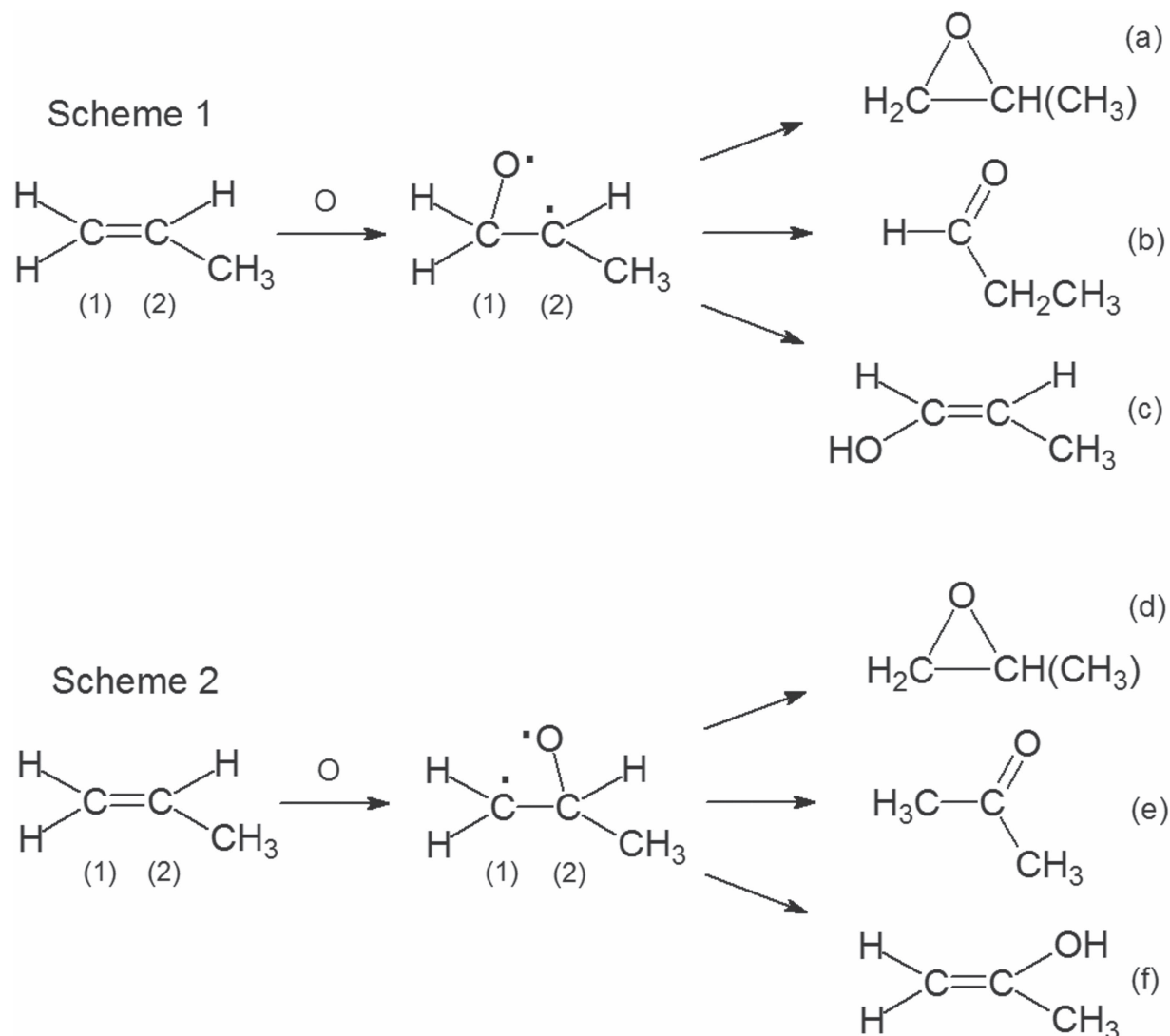


Figure 5. Oxygen-atom addition to propylene leads to two possible diradicals and to multiple product molecules depending on whether carbon (1) or (2) is the site of the addition. The product molecules shown are (a) propylene oxide, (b) propanal, (c) 2-methyl vinyl alcohol, (d) propylene oxide, (e) acetone, and (f) 1-methyl vinyl alcohol. Product (c) exists in two forms, designated Z when the OH and CH₃ groups are both below a horizontal line defined by the C=C bond, as drawn here, or designated E when they are on opposite sides (not shown) of the same.

Occhiogrosso et al. 2012). Mass spectral methods detected the release of reaction products and suggested that $O + C_2H_4 \rightarrow C_2H_4O$ occurs at 12–70 K, with the most abundant product being ethylene oxide. Arguing from analogous C_2H_4 experiments, mass spectral detections from $O + C_3H_6 \rightarrow C_3H_6O$ were suggested to indicate propylene oxide formation, but no unambiguous, direct PrO observation was possible. Our own work differs in that ices were irradiated, followed by in situ IR observations of PrO in the samples.

As this paper was being written, a combined laboratory and computational study by Abplanalp et al. (2016) appeared, directly addressing the formation, from CO and selected hydrocarbons, of several C_3H_6O isomers, but not propylene oxide. We agree with the main points of this recent paper, adding only that we now have shown that entry into the C_3H_6O family also is feasible in ices near 10 K through radiation-initiated O-atom addition, with the C_3 products observed and proposed in the present paper matching those of Abplanalp et al. (2016, Figure 1), aside from our PrO observation. We strongly agree with those same authors' overarching

conclusions about the ability of ionizing radiation to produce the variety and abundances of organic molecules observed in the interstellar medium.

4.3. Astrochemical Connections

An immediate result from this work is that another fruitful source of interstellar molecules has been uncovered. The argument we have used in the past is that “If X is interstellar then lab experiments imply that Y will be too.” With this argument we successfully predicted the discovery of both ketenimine and ethylene glycol as interstellar molecules (Hudson & Moore 2000, 2004). For propylene oxide, its recent detection and identification (McGuire et al. 2016) can be coupled to our new experiments to predict that the alcohols shown in Figure 5 should be present in the interstellar medium, as should methylketene, these molecules being formed on icy grains and, perhaps, ejected into the gas phase. An important restriction for gas-phase detections of vinyl alcohols is that these molecules are unstable with respect to rearrangement to make aldehydes and ketones, which probably explains why

they went undetected in the 1000 K shock experiments of Lifshitz & Tamburu (1994).

In this paper we have shown how propylene oxide can be made in an icy solid by radiation exposure, such as to MeV protons. Since the energy of keV and MeV radiations acting on molecular solids is dissipated by thousands of secondary electrons, with a mean energy near 10 eV (e.g., Pimblott & LaVerne 2007), then the reactions we report here are fully expected to occur on far-UV photolysis of the same ices. Therefore the formation of propylene oxide will occur and its reaction products will exist (Figure 5) in interstellar clouds with a wide range of opacities and energy inputs. In fact, the two stable carbonyl products of PrO in Figure 4, propanal and acetone, already are known to be interstellar, having been found, like propylene oxide, in Sagittarius B2 (Combes et al. 1987; Snyder et al. 2002; Hollis et al. 2004).

Our method for making interstellar propylene oxide could be just one of several routes to this molecule, but it is the only one so far demonstrated to occur at low temperatures. The reactants we selected, CO₂ and propylene, were chosen because they are known interstellar molecules, but other reactants are possible. Figure 2 shows that a fluence of about $1.2 \times 10^{13} p+ cm^{-2}$, corresponding to an absorbed dose of only about 0.24 eV molecule⁻¹, made an observable amount of PrO, from which we conclude that the radiation-driven $O + C_3H_6 \rightarrow C_3H_6O$ reaction can be relied on to make propylene oxide at low temperatures in icy solids. More specifically, for a dense cloud lifetime of $\sim 10^7$ years, the calculated cosmic-radiation dose is about 3 eV per H₂O molecule (Jenniskens et al. 1993; Moore et al. 2001), or about 7 eV per CO₂ molecule. This dose is more than enough to cover the results presented here as it corresponds to $\sim 4 \times 10^{14} p+ cm^{-2}$, greater than the horizontal axis of Figure 3's lower panel.

As for solar system chemistry, experiments have shown that ethylene oxide is made in simulations of Titan's atmospheric chemistry (Coll et al. 2003). As propylene has been detected at Titan (Nixon et al. 2013), it can act as an O-atom scavenger to make propylene oxide, and from there to other products. Also, to the degree that comets incorporate interstellar matter then similar chemistry should be preserved in them. We also suggest that chemical reactions resembling those reported here will occur during the alteration by UV photons of ices in a circumstellar disk or solar nebula, from which the reaction products could be incorporated into meteoritic material (Throop 2011; Ciesla & Sandford 2012). Our results might also find application to studies of trans-Neptunian objects. Earlier observations of Pluto's surface suggested the presence of hydrocarbon solids (Sasaki et al. 2005). It should now be possible to investigate whether propylene oxide might also be present, formed by radiation-induced reactions. Finally, the thermal stability we observed on warming frozen propylene oxide means that if delivered by comets or meteors to such closer objects as the Earth's moon or Mercury then it might remain trapped in permanently shadowed regions near each world's poles.

5. Conclusions

Infrared spectra of solid propylene oxide showed that it is stable against sublimation when warmed from 10 to ~ 130 K, and to at least 150 K after irradiation in CO₂. Two crystalline forms of propylene oxide were observed, and approximate transition temperatures recorded. A refractive index was

measured for amorphous propylene oxide, which led to a density estimate. Infrared band strengths were determined for amorphous propylene oxide, as were IR absorption coefficients. A radiation-chemical synthesis to make propylene oxide at 10 K was identified, and found to make detectable amounts of the compound even at low doses. This synthesis was tested with two sets of starting materials and by ¹⁸O isotopic substitution. The decomposition of propylene oxide was examined briefly. These new results lead to better characterization of solid propylene oxide, to predictions of methylketene and three vinyl alcohols as interstellar molecules, undetected to date, and to expectations of propylene oxide in multiple planetary environments.

Support for all authors through NASA Goddard's DREAM2 center, funded by NASA's SSERVI program, is acknowledged. The participation of K.M.Y. was made possible by a DREAM2 summer internship. Additional support for R.L.H. was provided by the NASA Astrobiology Institute's Goddard Center for Astrobiology and a grant from NASA's Cassini Data Analysis Program.

References

- Abplanalp, M. J., Gozem, S., Krylov, A. I., et al. 2016, *PNAS*, 113, 7727
 Andrews, L., & Kohlmler, C. K. 1982, *JPhCh*, 86, 4548
 Bennett, C. J., Osamura, Y., Lebar, M. D., & Kaiser, R. I. 2005, *ApJ*, 634, 698
 Ciesla, F. J., & Sandford, S. A. 2012, *Sci*, 336, 452
 Coleman, B. E., & Ault, B. S. 2010, *JMoSt*, 976, 249
 Coll, P., Bernard, J.-M., Navarro-González, R., & Raulin, F. 2003, *ApJ*, 598, 700
 Combes, F., Gerin, M., Wooten, A., et al. 1987, *A&A*, 180, L13
 Cvetanović, R. J. 1958, *CaJCh*, 36, 623
 Dickens, J. E., Irvine, W. M., Ohishi, M., et al. 1997, *ApJ*, 489, 753
 Dubnikova, F., & Lifshitz, A. 2000, *JPhCh*, 104, 4489
 Gerakines, P. A., & Hudson, R. L. 2013, *AsBio*, 13, 647
 Gerakines, P. A., & Hudson, R. L. 2015a, *ApJL*, 805, L20
 Gerakines, P. A., & Hudson, R. L. 2015b, *ApJL*, 808, L40
 Gilmore, W., Morris, M., Palmer, P., et al. 1976, *ApJ*, 204, 43
 Gontrani, L., Nunziante Cesaro, S., Stranges, S., Bencivenni, L., & Pieretti, A. 2014, *AcSpe*, 120, 558
 Groner, P., Stolkin, I., & Günthard, H. H. 1973, *JPhE*, 6, 122
 Guillory, W. A., & Thomas, S. G., Jr. 1975, *JPhCh*, 79, 692
 Hawkins, M., & Andrews, L. 1983, *JChS*, 105, 2523
 Holden, R. F. 1952, in *Glycols*, ed. G. O. Curme (New York: Reinhold), 250 Ch. 11
 Hollenberg, J., & Dows, D. A. 1961, *JChPh*, 34, 1061
 Hollis, J. M., Jewell, P. R., Lovas, F. J., Remijan, A., & Mollendal, H. 2004, *ApJL*, 610, L21
 Hudson, R. L., Ferrante, R. F., & Moore, M. H. 2014a, *Icar*, 228, 276
 Hudson, R. L., Gerakines, P. A., & Loeffler, M. J. 2015, *PCCP*, 17, 12545
 Hudson, R. L., Gerakines, P. A., & Moore, M. H. 2014b, *Icar*, 243, 148
 Hudson, R. L., & Loeffler, M. J. 2013, *ApJ*, 773, 1
 Hudson, R. L., & Moore, M. H. 2000, *Icar*, 145, 661
 Hudson, R. L., & Moore, M. H. 2003, *ApJL*, 586, L107
 Hudson, R. L., & Moore, M. H. 2004, *Icar*, 172, 466
 Jenniskens, P., Baratta, G. A., Kouchi, A., et al. 1993, *A&A*, 273, 583
 Katsuki, T., & Sharpless, K. B. 1980, *JChS*, 102, 5976
 Kwiatkowski, J. S., & Leszczyński, J. 1995, *JMoSt*, 342, 43
 Lifshitz, A., & Tamburu, C. 1994, *JPC*, 98, 1161
 Loeffler, M. J., Hudson, R. L., Chanover, N. J., & Simon, A. A. 2016a, *Icar*, 271, 265
 Loeffler, M. J., Moore, M. H., & Gerakines, P. A. 2016b, *ApJ*, 827, 985
 McGuire, B. A., Carroll, P. B., Loomis, R. A., et al. 2016, *Sci*, 352, 1449
 Moore, M. H., Ferrante, R. F., Moore, W. J., & Hudson, R. L. 2010, *ApJS*, 191, 96
 Moore, M. H., Hudson, R. L., & Gerakines, P. A. 2001, *AcSpe*, 57A, 843
 Nixon, C. A., Jennings, D. E., Bézard, B., et al. 2013, *ApJL*, 776, L14
 Occhiogrosso, A., Viti, S., Ward, M. D., & Price, S. D. 2012, *MNRAS*, 427, 2450
 Pimblott, S., & LaVerne, J. 2007, *RaPC*, 76, 1244
 Pileschajew, N. 1909, *BBGPC*, 42, 4811

Sasaki, T., Kanno, A., Ishiguro, M., Kinoshita, D., & Nakamura, R. 2005, *ApJL*, **618**, L57
Schriver, A., Coanga, J. M., Schriver-Mazzuoli, L., & Ehrenfreund, P. 2004, *CP*, **303**, 13
Snyder, L. E., Lovas, F. J., Mehringer, D. M., et al. 2002, *ApJ*, **578**, 245
Tempelmeyer, K. E., & Mills, D. W. 1968, *JAP*, **39**, 2968
Throop, H. B. 2011, *Icar*, **212**, 885

Tobin, M. C. 1960, *AcSpe*, **16**, 1108
Turner, B. E., & Apponi, A. J. 2001, *ApJL*, **561**, L207
Ward, M. D., & Price, S. P. 2011, *ApJ*, 741, 2011
Wilsmore, N. T. M., & Stewart, A. W. 1907, *Natur*, **75**, 510
Winther, F., Meyer, S., & Nicolaisen, F. 2002, *JMoSt*, **611**, 9
Ziegler, J. F. 2013, Stopping and Range of Ions in Matter SRIM2, 013
(available at www.srim.org)